

CONF-9606116--15

ANALYTICAL AND NUMERICAL MODELS OF URANIUM IGNITION  
ASSISTED BY HYDRIDE FORMATION

by

Terry C. Totemeier and Steven L. Hayes

Engineering Division  
Argonne National Laboratory-West  
P.O. Box 2528  
Idaho Falls, ID 83403-2528

RECEIVED  
APR 17 1996  
OSTI

The submitted manuscript has been authored by a contractor of the U. S. Government under contract No. W-31-109-ENG-38. Accordingly, the U. S. Government retains a nonexclusive, royalty-free license to publish or reproduce the published form of this contribution, or allow others to do so, for U. S. Government purposes.

Paper to be submitted for publication for  
The 1996 DOE Spent Nuclear Fuel and Fissile Material Management Conference  
Reno, Nevada

June 16-20, 1996

Work supported by the U.S. Department of Energy, Reactor Systems, Development and Technology, under Contract W-31-109-Eng-38.

DISTRIBUTION OF THIS DOCUMENT IS UNLIMITED

at  
**MASTER**

ANALYTICAL AND NUMERICAL MODELS OF URANIUM IGNITION  
ASSISTED BY HYDRIDE FORMATION

Terry C. Totemeier  
Argonne National Laboratory  
Idaho Falls, ID 83403-2528  
(208) 533-7458

Steven L. Hayes  
Argonne National Laboratory  
Idaho Falls, ID 83403-2528  
(208) 533-7255

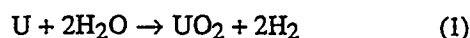
## ABSTRACT

Analytical and numerical models of uranium ignition assisted by the oxidation of uranium hydride are described. The models were developed to demonstrate that ignition of large uranium ingots could not occur as a result of possible hydride formation during storage. The thermodynamics-based analytical model predicted an overall 17°C temperature rise of the ingot due to hydride oxidation upon opening of the storage can in air. The numerical model predicted locally higher temperature increases at the surface; the transient temperature increase quickly dissipated. The numerical model was further used to determine conditions for which hydride oxidation does lead to ignition of uranium metal. Room temperature ignition only occurs for high hydride fractions in the nominally oxide reaction product and high specific surface areas of the uranium metal.

## I. INTRODUCTION

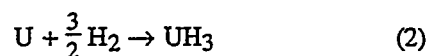
The expected interim- to long-term storage of significant quantities of uranium (as both metal feedstock and spent nuclear fuel) has led to a need for increased understanding of its storage behavior. For the metallic form, the principal concern is degradation due to oxidation and corrosion during storage, and the possibility of pyrophoric events during storage or subsequent handling after storage. Early experience with uranium metal<sup>1</sup> highlighted the strong role that uranium hydride can play in the ignition of uranium. Subsequent studies of both uranium and plutonium metal have verified that hydride formed during storage can increase their pyrophoric tendencies<sup>2</sup>.

Uranium metal reacts with water vapor to form uranium dioxide and hydrogen gas according to the reaction:



It is generally found that less than the stoichiometric amount of hydrogen gas is formed in this reaction; most researchers report the presence of uranium hydride (UH<sub>3</sub>) in the oxide reaction product to account for the remainder of the hydrogen<sup>3-6</sup>. There is little consistency as to the exact percentage of UH<sub>3</sub> formed—reported values range from 2%<sup>4</sup> to 30%<sup>6</sup>. The formation of higher percentages appears to be limited to crevice-type corrosion situations where there is restricted access of the ambient environment to the reaction product.

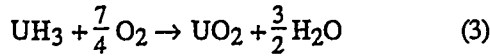
In a sealed canister storage situation it is theoretically possible to reach even higher hydride levels in the reaction product through a "recycling" mechanism whereby the hydrogen gas formed in reaction (1) and trapped in the canister further reacts with uranium metal:<sup>7</sup>



The percentage of hydride that would be present in a uranium-water vapor reaction product assuming that all hydrogen reacted to form hydride and no oxygen was present to form additional oxide is 57 mol% (from stoichiometry). Any additional sources of hydrogen gas, such as radiolysis of organic materials in the storage can,<sup>8</sup> could further increase the hydride fraction.

The potential for a pyrophoric incident is greatest upon opening of a canister which has been in storage.

The uranium hydride formed during storage will be stable until the canister is opened and air is re-admitted (assuming the canister is opened in air). Uranium hydride is reported to be pyrophoric in the presence of air and will burn even at room temperature according to the reaction:<sup>9</sup>



This reaction liberates a significant amount of heat, 1,386 kJ/mol  $\text{UH}_3$ . Such rapid heat generation on the surface of the remaining uranium may be sufficient to initiate pyrophoric burning of the metal.

This paper describes the development and results of analytical and numerical models of uranium ignition assisted by rapid oxidation of uranium hydride. The analytical model considers the temperature rise of a uranium ingot due to the oxidation of hydride formed during storage using conservative assumptions. The numerical model is used to further investigate this phenomenon for spherical particles with varying surface areas, amounts of reaction product, and hydride fractions in the reaction product.

## II. ANALYTICAL MODEL

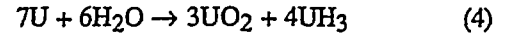
The impetus for the development of a simple analytical model of the effect of uranium hydride on the ignition behavior of uranium metal was the storage of uranium ingots produced in the electrometallurgical process for stabilizing spent nuclear fuel currently being developed at Argonne National Laboratory (ANL). These ingots may be interim stored on-site until final disposition is decided and executed, a period of up to 50 years. This model was intended to provide a safety calculation to insure that any hydride formed during storage will not cause ignition of the stored uranium upon re-opening (either intentionally or by accident).

The first step in the analysis is the calculation of the amount of uranium hydride which could be formed during extended storage. To make this calculation, it was assumed that the amount of gas in the storage canister is fixed and no leaks are present. The storage cans will be seal welded and leak checked, so this is a reasonable assumption. The effect of any leak can be determined by multiplying the maximum expected leak rate by the storage time to determine the amount of gas admitted.

We further assumed that all of the hydrogen present in the canister (as water vapor) at the time of seal welding reacts with uranium during storage to form uranium

hydride according to reactions (1) and (2) above. The initial storage gas is assumed to be ambient air.

The number of moles of hydride that can be formed from a given quantity of water is determined by the stoichiometry of the net water-to-hydride reaction:



hence

$$n_{\text{UH}_3} = \frac{2}{3} n_{\text{H}_2\text{O}} \quad (5)$$

where  $n_i$  are the number of moles of a given reactant. The molar quantity of any species in the storage gas is given by the ideal gas law:

$$n_i = \frac{PV_{\text{gas}}}{RT} x_i \quad (6)$$

where  $x_i$  is the concentration of a species in the gas,  $P$  is the ambient pressure,  $V_{\text{gas}}$  is the volume of gas space in the canister (the volume of the canister minus the uranium volume),  $R$  is the gas constant, and  $T$  is the absolute temperature. Substitution of equation (6) into equation (5) yields the following expression:

$$n_{\text{UH}_3} = \frac{2}{3} \frac{PV_{\text{gas}}}{RT} x_{\text{H}_2\text{O}} \quad (7)$$

The amount of uranium metal present in the container is reduced by reaction (4) and by the reaction of uranium with oxygen present in the gas to form  $\text{UO}_2$ . The amount of uranium remaining after the reactions is:

$$n_{\text{U}} = n_{\text{U}_0} - \frac{7}{6} n_{\text{H}_2\text{O}} - n_{\text{O}_2} \quad (8)$$

where  $n_{\text{U}_0}$  is the original number of moles of uranium.

When the canister is opened and the hydride is oxidized according to reaction (3), an amount of heat equal to  $\Delta H \cdot n_{\text{UH}_3}$  will be released, where  $\Delta H$  is the enthalpy change of reaction (3). If it is assumed that this heat creates a uniform temperature increase in the uranium metal and all heat produced goes toward heating the uranium (adiabatic process), the temperature increase can be computed using the molar specific heat of uranium,  $C_p$ :

$$\Delta T = \frac{-\Delta H \cdot n_{\text{UH}_3}}{n_{\text{U}} \cdot C_p} \quad (9)$$

where  $\Delta T$  is the temperature increase. Substitution of equation (7) for  $n_{UH_3}$ , equation (8) for  $n_U$ , and simplification using the ideal gas law yields the following relationship:

$$\Delta T = \frac{\frac{2}{3} \frac{PV_{\text{gas}}}{RT} (x_{H_2O}) (-\Delta H)}{C_p \left[ n_{U_0} - \frac{PV_{\text{gas}}}{RT} (x_{O_2} + \frac{7}{6} x_{H_2O}) \right]} \quad (10)$$

This expression provides a relationship between the expected temperature rise of a uranium ingot due to hydride oxidation and the initial storage gas volume, pressure, and composition. Additional hydride formed as a result of any leakage of the canister can be incorporated into the temperature rise by an additional term in equation (10):

$$\Delta T = \frac{\frac{2}{3} \frac{P(V_{\text{gas}} + Qt)}{RT} (x_{H_2O}) (-\Delta H)}{C_p \left[ n_{U_0} - \frac{P(V_{\text{gas}} + Qt)}{RT} (x_{O_2} + \frac{7}{6} x_{H_2O}) \right]} \quad (11)$$

where  $Q$  is the volumetric leak rate and  $t$  is the storage time. Equation (11) is valid under the assumption that the leak gas has the same pressure and composition as the initial storage gas.

Equation (10) was used to compute the expected temperature rise due to hydride oxidation for the anticipated storage of uranium ingots at the ANL-W site. The interior volume of the 30.5 cm diameter and 1.52 m long cylindrical canister is  $0.035 \text{ m}^3$ . Four 35 kg ingots of uranium will be stored in each canister, a total volume of  $0.028 \text{ m}^3$ . It was conservatively assumed that only one ingot of the four will have reacted with the gas to form hydride, so the initial starting mass of uranium was 35 kg (147 moles). The molar specific heat of uranium is  $27.67 \text{ J/K}\cdot\text{mol}$ .<sup>10</sup> The pressure and composition of the ambient air at the ANL-W site are 84.9 kPa and 20.9%  $O_2$ . The fraction of water vapor ( $x_{H_2O}$ ) was computed for humid conditions to be 0.78%.

Insertion of these values into equation (10) resulted in a  $17^\circ\text{C}$  temperature rise. Given the small specific surface area of the large ingots, it was readily apparent that this situation presents no risk of a pyrophoric incident, even for slightly elevated initial temperatures. However, there is one non-conservative assumption built into this analysis, namely that the heat of hydride oxidation is immediately distributed evenly throughout the ingot. Because the hydride oxidation reaction is pyrophoric (occurs very quickly) and the hydride is located on the

surface of the ingot, local temperature increases at the ingot surface may be much higher than  $17^\circ\text{C}$ . Higher surface temperatures of the ingot will give higher uranium oxidation rates, which in turn will generate heat ( $1,085 \text{ kJ/mol } UO_2$ ) and further raise temperatures. The kinetic questions raised in this scenario cannot be answered by the thermodynamic analytical model presented above. The next section describes the development of a numerical model to account for the kinetics of heat generation and removal.

### III. NUMERICAL MODEL

#### A. Model Description

The numerical model employs a transient, finite-difference based FORTRAN computer program to track the oxidation of a metal ingot and analyze its thermal response. To allow for ease of implementation, the numerical model was applied to the one-dimensional case of an isolated metal sphere rejecting heat to the environment by convection and radiation. Heat conduction is calculated on a numerical grid within the sphere, with heat generation occurring at the oxide-metal interface where the reaction is taking place. Thus, temperatures are known throughout the metal ingot, and the oxidation rate at the oxide-metal interface is calculated using the temperature of the interface. The computer program has been designated SPARC, for Spherical Particle Autothermic Reaction Code.

The numerical model requires the density, thermal conductivity, and specific heat for uranium and  $UO_2$ , the heat of formation of  $UO_2$ , and the oxidation rate equation for uranium. The rate equation employed in this analysis was that of Baker and Bingle<sup>11</sup> for the oxidation of uranium in  $O_2$ , as shown below.

For  $300 < T < 450^\circ\text{C}$ :

$$\frac{dw}{dt} = \frac{5}{4} w^{1/5} (1.0 \times 10^5) \exp \left[ \frac{-70,342}{RT} \right] \quad (12)$$

For  $T \geq 450^\circ\text{C}$ :

$$\frac{dw}{dt} = \frac{5}{6} w^{-1/5} (1.8 \times 10^4) \exp \left[ \frac{-59,874}{RT} \right] \quad (13)$$

where  $w$  is the quantity of oxygen reacted ( $\text{mg}/\text{cm}^2$ ),  $t$  is time (min),  $R$  is the gas constant ( $\text{J}/\text{mol}\cdot\text{K}$ ), and  $T$  is absolute temperature (K). These equations reflect the observation that above  $450^\circ\text{C}$  the uranium oxidation rate

slows as oxidation proceeds due to the buildup of a protective oxide layer that retards oxygen diffusion to the oxide-metal interface. No such dependence has been noted below 450°C; in fact the oxidation rates as measured by Baker and Bingle<sup>11</sup> have been seen to increase with reaction extent.

The model allows an initial reaction layer of a given thickness to be present on the surface of the sphere at the start of a calculation. The initial reaction layer is assumed nominally to be oxide, but can be specified to contain a given mole fraction of hydride. Any hydride present at the beginning of a calculation is assumed to oxidize according to reaction (3) during the first time step, which can be specified to be of any duration.

During the initial investigation of heavy oxidation of large ingots, it was found that a thick oxide layer insulated the ingot considerably and led to predicted ignition temperatures lower than the experimental data suggested. In reality, the oxide reaction product flakes or spalls off the metal ingot during the course of the reaction. To account for this phenomenon, a critical thickness of the reaction layer can be specified in the model. Once the reaction layer reaches this critical thickness, further inward oxidation occurs at the expense of an equivalent amount of oxide spalled off the outer surface of the ingot. Use of this spallation option has resulted in good agreement with experimental data for large ingots.

Calculations may be made with SPARC in one of two ways. A "burning curve" calculation may be made in which the ambient (furnace) temperature is ramped at a specified rate until ignition of the metal occurs, which mimics the procedure commonly employed experimentally. Ignition is identified as the temperature at which the time rate of change of a characteristic temperature (in this case the oxide-metal interface temperature) achieves a specified value. For the present work, that value has been taken to be 100°C/minute, as suggested by Musgrave.<sup>12</sup> Alternatively, an "isothermal" calculation can be made in which the ambient temperature remains at a fixed value. The ignition temperature is then defined as that ambient or furnace temperature that results in the metal ingot igniting. The two methods do not produce in the same ignition temperature under equivalent conditions, as discussed in the next section.

The model employs implicit time-marching with an under-relaxation of ~0.8 for solution stability; temperatures are converged to  $<10^{-4}$  during each time-step. The numerical solution to the heat conduction equation was verified against analytical solutions. The

next section describes the further validation of the model using experimental data on uranium ignition.

## B. Model Validation

The model was first run in the isothermal mode at a variety of temperatures to produce oxidation results in the form of weight gain as a function of time. In this way the model was shown to reproduce the simple oxidation data on which the empirical equations given in the previous section were based. Since the thrust of this work was to identify probable ignition conditions, validation of the model against ignition data was also needed.

Essentially all uranium ignition experimental data have been generated by the burning curve method. Cubic solids, wires and foils of uranium have been used in burning curve experiments to investigate a range of specific surface areas ( $\text{cm}^2/\text{g}$ ), a parameter on which the ignition temperature is strongly dependent. The SPARC model uses a spherical geometry; any specific surface area can be achieved by using spheres of variable diameters, but it is necessary to establish the validity of applying data generated by spherical calculations to other geometries.

Figure 1 shows the results of a series of calculations made using SPARC compared to the experimental data of Baker et al.<sup>13</sup> produced using the burning curve method. Baker et al. performed ignition tests in both air and  $\text{O}_2$ ; ignition temperatures are seen to be lower in  $\text{O}_2$  than in air.

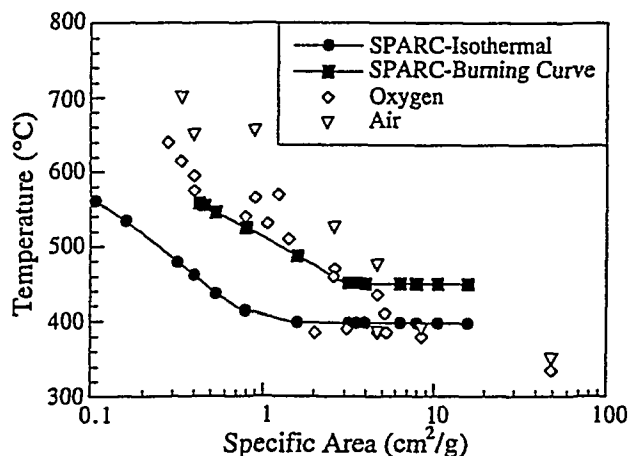


Figure 1: Validation of SPARC numerical model against experimental uranium burning curve experiments.

The burning curve results produced by SPARC are in good agreement with the experimental data obtained in  $O_2$  up to a specific area of about  $3 \text{ cm}^2/\text{g}$ . At this point, the ignition temperatures calculated by SPARC flatten off at a constant value, while the experimental data continues to decrease. The experimental data above  $3 \text{ cm}^2/\text{g}$  were generated with foils. The spheres used in the model calculations for this specific surface area regime became very small ( $<0.1 \text{ cm}$ ). So while the specific areas of the very small spheres and the foils were similar, the foil samples were much more massive, with the greater thermal mass leading to lower ignition temperatures. This represents a regime in which the spherical data and foil data do not correlate the same with specific surface area. However, for specific surface areas below  $3 \text{ cm}^2/\text{g}$ , the correlation is very good.

Also shown in Figure 1 are similar results obtained using SPARC's isothermal mode to locate the ignition temperature. Use of the isothermal mode results in ignition temperatures significantly lower than those obtained from burning curve calculations, a difference which has been noted experimentally by Schnizlein, et al.<sup>14</sup> The isothermal method has not been generally employed experimentally because of the large number of samples that would be required to locate the ignition temperature with any precision. However, the isothermal methodology is not difficult to implement using model calculations, and it is regarded as providing an ignition temperature more reflective of actual conditions. The ignition temperatures presented in the next section were located using the isothermal method.

### C. Model Calculations

The first analysis undertaken with a validated numerical model was that of the 35 kg uranium storage ingot previously analyzed using the analytical model. A 10.6 cm diameter sphere of uranium was calculated to have the same specific area as the intended cylindrical ingot,  $0.03 \text{ cm}^2/\text{g}$ . The reaction of the uranium metal with storage gases under the assumptions described for the analytical model above produces a  $43 \mu\text{m}$  thick reaction product of 80 mol%  $UO_2$  and 20 mol%  $UH_3$ . A natural convection heat transfer coefficient of  $0.002 \text{ W}/\text{cm}^2\cdot\text{K}$  and an emissivity of 0.8 for  $UO_2$  were used in the model calculations.

Since the kinetics of the hydride oxidation reaction are known to be very rapid, it was assumed that the energy from this reaction was deposited into the  $UO_2$  reaction product during the first 0.1 second. Once the hydride oxidizes, the reaction product will be composed entirely of

$UO_2$ . The resulting temperature rise of the oxide-metal interface was calculated to be  $206^\circ\text{C}$ , significantly higher than the bulk temperature rise calculated from the analytical model. However, ignition did not occur and the metal ingot cooled to essentially room temperature within 30 seconds. Figure 2 shows the variance of oxide-metal interface and centerline temperatures with time after the oxidation of the hydride occurs.

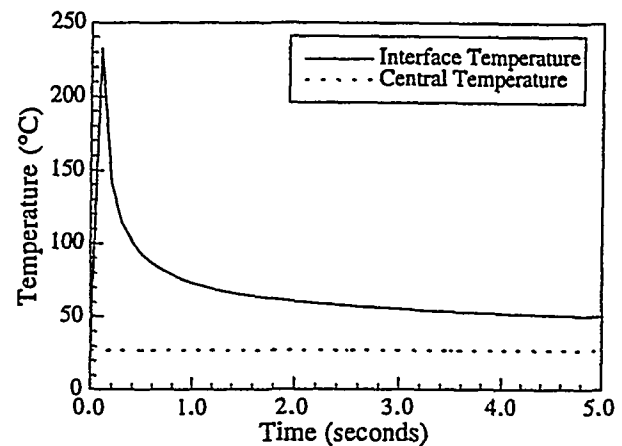


Figure 2: Variation of oxide-metal interface and centerline temperatures with time after hydride oxidation on a large uranium ingot.

The results of this calculation confirm that there are no ignition hazards associated with the proposed storage form. However, having a versatile numerical ignition model allows for the investigation of conditions under which ignition hazards may exist. Such an investigation was undertaken by calculating ignition temperatures for spheres having specific surface areas of  $0.08$  to  $10 \text{ cm}^2/\text{g}$  (diameters from 4 to  $0.03 \text{ cm}$ ), initial reaction layer thicknesses of 10 to  $100 \mu\text{m}$ , and hydride fractions of 5 to 57 mol%.

Diagrams showing regions where the numerical model predicts that oxidation of a surface layer of uranium hydride results in ignition of a uranium metal particle were constructed using the data from the parametric study. Two ambient temperatures were considered, room temperature and  $100^\circ\text{C}$ . Room temperature represents the case of normal opening of the storage canister in air, while  $100^\circ\text{C}$  represents the opening of the canister at a more elevated temperature in a possible accident scenario. For each temperature and a given hydride fraction in the reaction product, parametric combinations of product thickness and uranium particle specific area were plotted,

with each point marked to signify whether the model determined that ignition had occurred for that condition. A curve was then drawn along the boundary between points which showed ignition and those that did not. This process was repeated at each temperature for a total of four hydride fractions (5%, 10%, 30%, and 50%).

Figure 3 shows the curves determined for room temperature; Figure 4 shows the curves for 100°C. For a particular fraction of hydride in the reaction product (a particular curve), the numerical model predicts ignition in the region above and to the right of the curve; ignition is not predicted for the region below and to the left of the curve. For example, consider the room temperature air exposure of a particle 2 mm in diameter with 60  $\mu\text{m}$  of reaction product on the surface. On Figure 3, the thickness/specific area combination of this particle would lie between the line labeled 30% and the line labeled 10%. For this condition the model predicts ignition of the particle if the hydride fraction in the reaction product is greater than 30%, but no ignition if the fraction is less than 10%.

The variance of ignition conditions with the four variables considered (ambient temperature, product thickness, product hydride fraction, and uranium particle specific area) was as anticipated. Ignition has an increased tendency to occur with increasing product thicknesses and hydride fractions; larger amounts of product and hydride fractions produce larger initial heat inputs to the uranium metal particle. Increasing specific area decreases the standard ignition temperature of the uranium particle, hence lower heat inputs are necessary to heat the particle to ignition. The higher ambient temperature of 100°C reduces the temperature increase needed for a given particle to reach its ignition temperature and also reduces heat losses to the surroundings. This change in behavior is reflected by the shift of the curves to the left in Figure 4 as compared to Figure 3.

Close examination of Figure 3 and 4 reveals that ignition due to hydride oxidation is not a concern for bulk uranium pieces with reasonable levels of hydride fractions in the corrosion product (less than 10%). Bulk uranium pieces will have specific areas greater than 1  $\text{cm}^2/\text{g}$ . Ignition at that specific area is not predicted for 10% and 5% hydride fractions, even with product thickness of up to 100  $\mu\text{m}$ . However, these plots do show that room temperature ignition will be a serious concern for fine powders or for very high hydride fractions such as may be formed when excess hydrogen gas is present in the storage environment. Hydrogen gas may be generated by radiolysis of organic packing materials.<sup>8</sup>

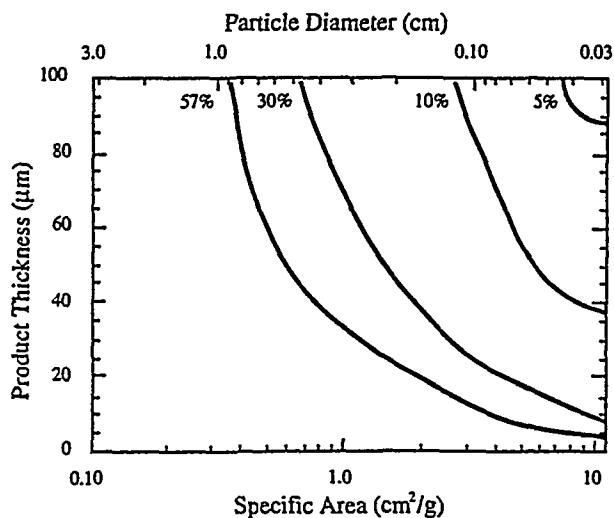


Figure 3: Map of room temperature ignition conditions as a function of product thickness, particle specific area, and reaction product uranium hydride fraction.

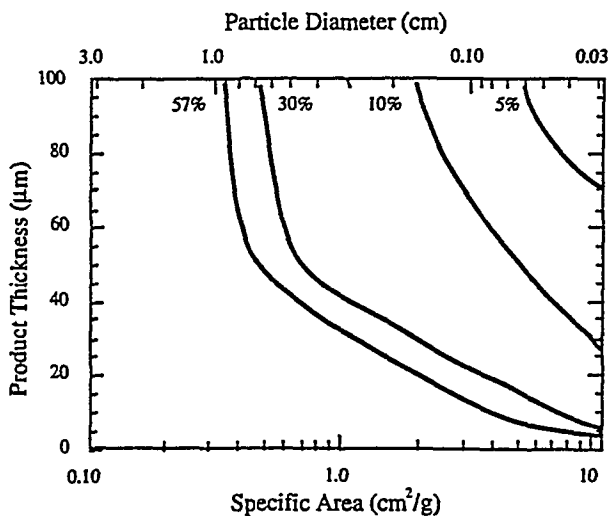


Figure 4: Map of 100°C ignition conditions as a function of product thickness, particle specific area, and reaction product uranium hydride fraction.

#### IV. CONCLUSIONS

The ignition of uranium metal assisted by the oxidation of uranium hydride formed during storage was examined using analytical and numerical models.

- A simple thermodynamic calculation was performed to relate the temperature rise of uranium pieces as a function of storage gas composition and canister

seal leak rate. A 17°C temperature rise was predicted for the anticipated storage of 35 kg ingots at ANL-W.

- A finite-difference based numerical model was developed to address the non-conservatism inherent in the thermodynamic calculation. Application of this model to the anticipated storage scenario revealed a greater extent of localized surface heating than calculated in the analytical model, but no ignition of the uranium ingot.
- The numerical model was further used to determine sets of conditions (ambient temperature, reaction product thickness and hydride fraction, and uranium particle specific area) for which ignition does occur. High hydride fractions and uranium particle specific areas are required for room temperature ignition to occur.

#### ACKNOWLEDGEMENTS

The authors wish to acknowledge the assistance and helpful criticism of R.G. Pahl and D.C. Crawford in the development of the models. This work was supported by the U.S. Department of Energy, Reactor Systems, Development and Technology, under contract W-31-109-Eng-38.

#### REFERENCES

1. R.B. Smith, *The Fire Properties of Metallic Uranium*, TID-8011, Technical Information Service, Atomic Energy Commission, Washington, D.C. (1956).
2. J.L. Stakebake, *Plutonium Pyrophoricity*, EG&G Rocky Flats Plant Technical Report RFP-4517 (1992).
3. T. Kondo, F.H. Beck, and M.G. Fontana, "A Gas Chromatographic Study on the Kinetics of Uranium Oxidation in Moist Environments," *Corrosion*, **30**, 330 (1974).
4. M.M. Baker, L.N. Less, and S. Orman, "Uranium and water reaction. Part I - Kinetics, Products, and Mechanism," *Trans. Faraday Soc.*, **62**, 2513 (1966).
5. K. Winer, C.A. Colmenares, R.L. Smith, and F. Wooten, "Interaction of Water Vapor with Clean and Oxygen-Covered Uranium Surfaces," *Surface Science*, **183**, 67 (1987).
6. R.V. Strain and J.M. Carpenter, "Examination of Disks from the IPNS Depleted Uranium Target," presented at the 13th Meeting of the International Collaboration on Advanced Neutron Sources, Oct. 11-14, 1995, Villigen, Switzerland (to be published).
7. C.W. Solbrig, J.R. Krsul, and D.N. Olsen, "Pyrophoricity of Uranium in Long-Term Storage Environments", in *DOE Spent Nuclear Fuel - Challenges and Initiatives*, p. 89, ANS, La Grange Park, IL, (1994).
8. G. Friedlander, J.W. Kennedy, and J.M. Miller, *Nuclear Radiochemistry*, 2nd ed., John Wiley and Sons, New York (1966).
9. J.J. Katz and E. Rabinowitch, *The Chemistry of Uranium - Part I*, p. 201, McGraw-Hill, New York (1951).
10. C.A. Hampel, ed., *The Encyclopedia of Chemical Elements*, p. 778, Reinhold Book Corporation, New York (1968).
11. L. Baker and J.D. Bingle, "The Kinetic of Oxidation of Uranium Between 300 and 625°C," *J. Nucl. Mater.*, **20**, 11 (1966).
12. L.E. Musgrave, A Theory of Burning Curve Ignition of Nuclear Materials," *J. Nucl. Mater.*, **43**, 155 (1972).
13. L. Baker, L.G. Schnizlein, and J.D. Bingle, "The Ignition of Uranium," *J. Nucl. Mater.*, **20**, 22 (1966).
14. J.G. Schnizlein, P.L. Pizzolato, H.A. Porte, J.D. Bingle, D.F. Fischer, L.W. Mishler, and R.C. Vogel, *Ignition Behavior and Kinetics of Oxidation of the Reactor Metals Uranium, Zirconium, Plutonium, and Thorium, and Binary Alloys of Each*, Argonne National Laboratory Technical Report ANL-5974 (1959).

## DISCLAIMER

This report was prepared as an account of work sponsored by an agency of the United States Government. Neither the United States Government nor any agency thereof, nor any of their employees, makes any warranty, express or implied, or assumes any legal liability or responsibility for the accuracy, completeness, or usefulness of any information, apparatus, product, or process disclosed, or represents that its use would not infringe privately owned rights. Reference herein to any specific commercial product, process, or service by trade name, trademark, manufacturer, or otherwise does not necessarily constitute or imply its endorsement, recommendation, or favoring by the United States Government or any agency thereof. The views and opinions of authors expressed herein do not necessarily state or reflect those of the United States Government or any agency thereof.